16th World Conference on Earthquake, 16WCEE 2017
Santiago Chile, January 9th to 13th 2017
Paper N0 °70 (Abstract ID)
Registration Code: S-D1463194061

DEVELOPMENT AND VALIDATION OF A SEISMIC RETROFIT SCHEME FOR REINFORCED CONCRETE BEAM-COLUMN JOINTS

Q. X. Huang[1], J S Kuang[2], Z. X. Guo[3], H. Behnam[4], Y. Liu[5]

[1] *Associate Professor, College of Civil Engineering, Huaqiao University, Xiamen, China.* haungqx@hqu.edu.cn
[2] *Professor, Dept. of Civil and Env. Eng., Hong Kong University of Science and Technology, Hong Kong.* cejkuang@ust.hk
[3] *Professor, College of Civil Engineering, Huaqiao University, Xiamen, China.* guozxy@hqu.edu.cn
[4] *PhD Candidate, Dept. of Civil and Env. Eng., Hong Kong University of Science and Technology, Hong Kong.* hbehnam@ust.hk
[5] *Associate Professor, College of Civil Engineering, Huaqiao University, Xiamen, China.* lyliuyang@hqu.edu.cn

Abstract

An innovative and efficient technique is presented for the seismic retrofit of reinforced concrete beam-column joints using prestressed high-strength steel wires (PHSW). This method is to improve the seismic performance and enhance the shear strength of beam-column joints with non-seismic design as well as to overcome the shortcomings of traditional seismic retrofitting techniques for the joints. Five interior beam-column joints that were tested under reversed cyclic loading. The specimens included one un-retrofitted control specimen and four strengthened joints using proposed PHSW technique including two joints without transverse beam and two with transverse beams.

Test results showed a significant increase in the joint shear capacity and reduction of the cracks on the joints in retrofitted specimens. In addition, energy dissipation and ductility level of beam-column joints were improved in retrofitted specimens compare to control specimen. The failure mode of the retrofitted specimens altered from brittle shear failure of beam-column joints to the ductile flexural failure. Meanwhile, no anchorage failures at lap splice locations of steel wire were observed in the tests. External retrofit technique proposed in this paper provides excellent tools to overcome the stress-lag between the retrofitted and the original part, by increasing the positive confinement around the joint.

Keywords: Beam-column joint, Seismic retrofit, Prestressed high-strength steel wire (PHSW), Seismic behavior, Cyclic load

1. Introduction

The shear failure of joints in moment-resistance frames induces severe structural damage and collapse of structures during strong earthquake. At the moment, there are still many frame structures designed and built without sufficient seismic considerations. These structures are seismically vulnerable due to inadequate or even no shear reinforcement within the beam-column joint. Hence, it is urgent to develop efficient retrofit technique to upgrade the joint's capacity of the existing buildings which do not meet the current seismic design requirements.

From the published literatures, several retrofit strategies for upgrading the beam-column joint can be found. These strengthening techniques are including: increasing sectional area of the joint [1-3], steel jackets [4-5], warping FRP [6-7], and combined strengthening [8-9]. These retrofitting methods have been confirmed to effectively improve the strength and ductility of beam-column joints. However, problems exist in the above mentioned retrofit techniques. (1) Some experimental studies ignore the obstacle of the slab and beams in the other direction, and hence it is difficult to practically apply these retrofit methods to both interior and exterior joints in buildings. (2) Because of the obstacle of beams in the other direction, effective confinement to the joint cannot be developed, and hence it is difficult to anchor the steel reinforcement. (3) The severe stress-lag between the retrofitted part and the original part usually exists, which will reduce the reinforcement effect. For example de-bonding effect in FRP application is one of the major shortcomings of the application of the FRP sheets.

It is well known that external pre-stressing can overcome the stress-lag between the retrofitted part and the original part. External pre-stressing increases the positive confinement and improves the reinforcement effect. The concrete columns retrofitted by external pre-stressing were investigated by prior researchers [10-12]. Their experimental results indicated that lateral external pre-stressing of concrete column is a viable seismic retrofitting technique which can effectively enhance the shear strength and ductility capacity of the column. However, these seismic retrofit techniques for columns using lateral external pre-stressing could not overcome the obstacle of transverse beams connected to the joint, and thus, cannot apply it to the beam-column joint.

The objective of this paper is to develop an innovative and efficient, yet economic, retrofit technique to improve the seismic performance and enhance the shear capacity of beam-column joints. Based on the principle of the transverse external pre-stressing technique, a new seismic retrofit procedure for RC beam-column joints is proposed using pre-stressed high-strength steel wires (PHSW). Since the steel wire has high yield strength and is ductile as well as corrosion resistant, it is very suitable for a use of wrapping around beam-column joints, thus effectively providing lateral confinement to the joints.

2. Experimental programme

2.1 Joint retrofit scheme

The seismic retrofit scheme for shear reinforcement deficient interial joint using PHSW is presented in Fig. 1. The concept of the retrofit scheme is using the high-strength and ductile material and external pre-stressing technique to improve the seismic performance and enhance the shear capacity of beam-column joint. High-strength steel wires are wrapped around the joint through the hole drilled in the depth of beams and applied prestressing force, as shown in Fig.1.

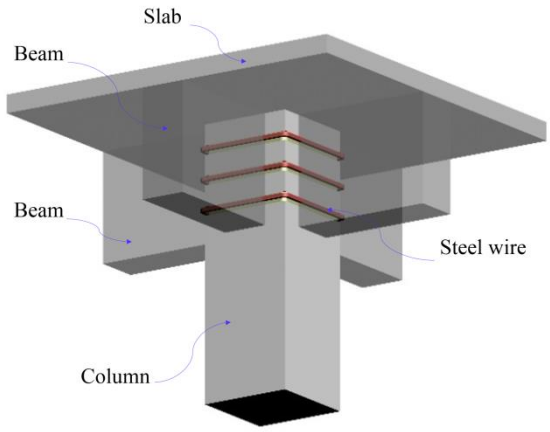

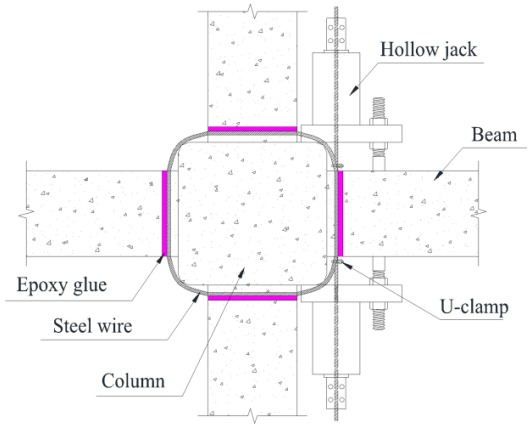

(a) Drilling holes and rounding corners

(b) Applying prestressing force

(c) Injecting epoxy glue

(d) Plastering polymer mortar layer

Fig. 1- Retrofit scheme using PHSW

The retrofit procedure is listed as follow: Prior to retrofitting, holes were drilled and cleaned using an air compressor at the pre-decided locations, and then the corners of the square column were rounded. Steel pieces were cut from a steel pipe of 50 mm diameter and placed over the column corners to avoid stress concentration and the resulting crushing of concrete at these locations, as shown in Figure 1(a). After inserting the steel wires through the holes, prestressing force was applied using two sets of hollow jacks shown in Figure 1(b). Once the hydraulic pressure reached the expected value, the high-stregnth steel wire was anchored using a special clip. Epoxy glue was then applied to fill the holes, as shown in Figure 1(c), to strengthen the anchorage effect of lap splices. Finally, the retrofitted specimens were plastered using a polymer mortar layer in the retrofitted region, as shown in Figure 1(d).

2.2 Test specimens

The experimental programme consisted of five full-scale interior beam-column joint subassemblages that were considered to be isolated from an existing typical RC frame building having an inter-storey height of 3.6 meters and a beam with an effective span of 4.8 meters. The joints were designed assuming that the points of contraflexure occur at midheight of the columns and midspan of the beams. To investigate the efficiency and effectiveness of the new retrofit scheme, the specimens included one control specimen, two planar joints and two spatial joints. The original specimens were designed in terms of strong-column/weak-beam concept, and the joint representing a deficient joint was expected to fail in brittle shear mode under reverse cycle loading. The joints have the identical dimensions, reinforcement details and material properties. Considering the test setup, the subassemblages have the following general and cross-sectional dimensions: column height of 1686 mm and beam length of 2600 mm with cross-sections of (250×250) mm and (150×300) mm, respectively. The spatial joints were constructed with transverse beams in two sides to investigate the effect of lap splice locations of PHSW. The length of transverse beams are 500mm with cross-sections of (150×300) mm. The dimensions of the specimens are shown in Fig. 2.

The PHSW ratio, prestressing level and polymer mortar of the test specimens are shown in Table 1. Prestressing level was defined as the ratio of pre-tensioning force to the maximum load of high-strength steel wire (HSW). Strengthening configuration can be reflected as the ratio of HSW in the joint region, which is defined as cross-sectional area of HSW ($A_{sv,j}$) to the product of column width b_c and beam depth h_b. The concept of the retrofit scheme is using the high-strength, flexible material properties and positive confinement effect to enhance the shear resistance capacity of beam-column joint. The retrofit technology using PHSW can artfully overcome the obstacle of the beams connecting with joint and eliminate or mitigate the leg-stress effect.

Table 1- Test specimens

Specimen	HSW configuration in joint region	Ratio of HSW in joint region (%)	Polymer mortar layer(mm)	Prestressing level	Type of joint	Anchorage location
J1	-		-	-	Planar joint	Fig.3a
J2	2D6 @100	0.064	-	0.3	Planar joint	Fig.3a
J3	2D6 @100	0.064	25	0.3	Planar joint	Fig.3a
J7	2D6 @100	0.064	25	0.3	Spatial joint	Fig.3b
J8	2D6 @100	0.064	25	0.3	Spatial joint	Fig.3c

2.3 Material properties

All test specimens were constructed using normal weight and ready mixed concrete with targeted 28-day concrete compressive strength of 21.4 MPa. Mechanical properties of the steel reinforcement for 6 mm, 14 mm

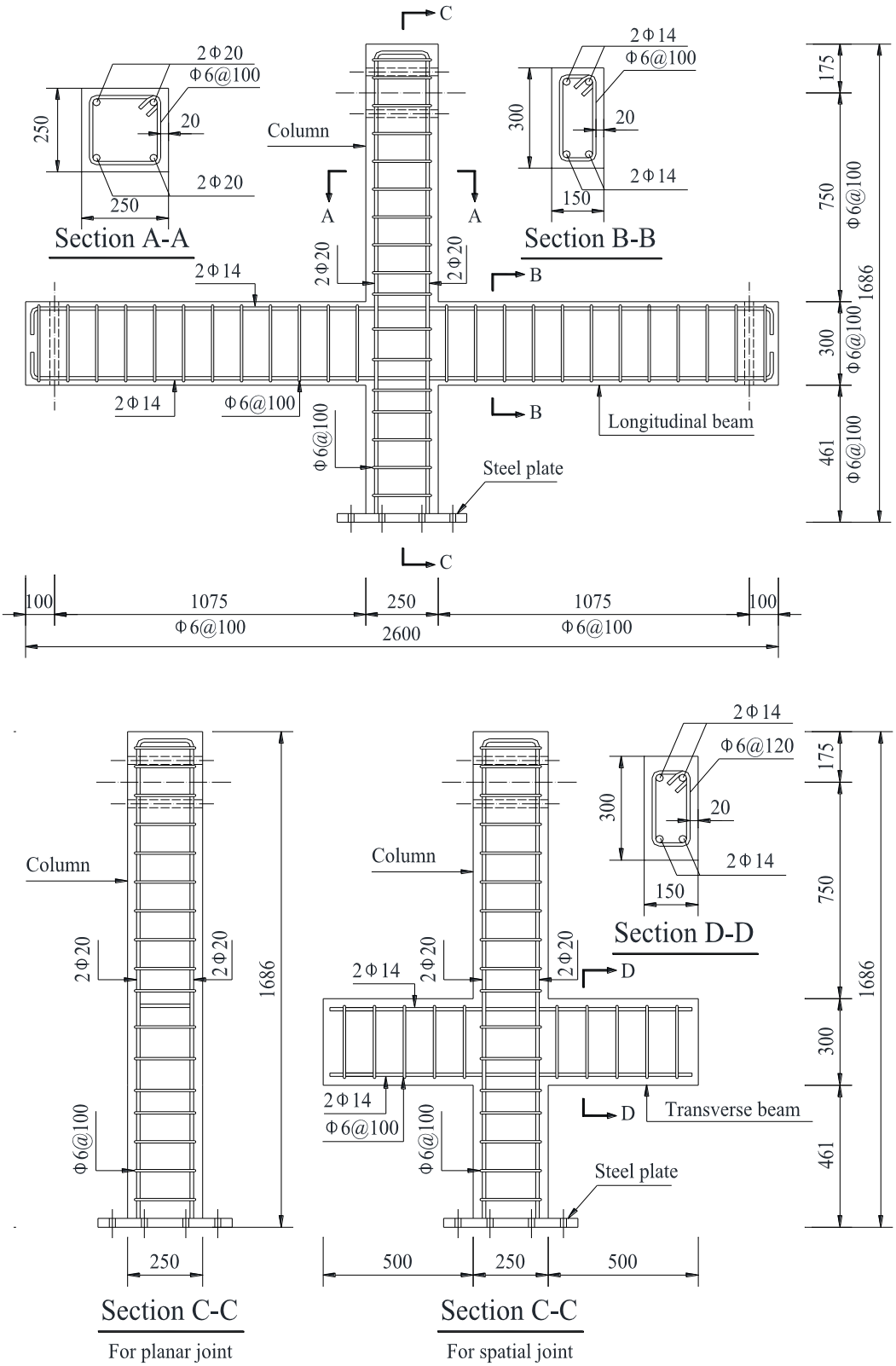

Fig.2-Dimensions and reinforcement details of original specimens (dimensions in mm)

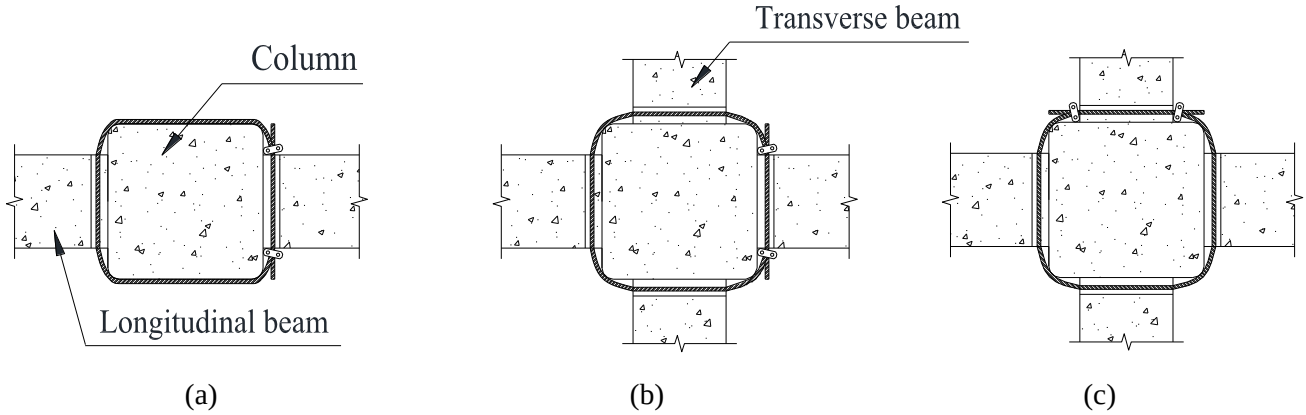

Fig.3- Anchorage location of PHSW

and 20 mm diameters are shown in Table 2. The mechanical properties of steel wire rope are shown in Table 3. The compression and tensile strength of epoxy glue, used for filling the holes drilled in the beams to strengthen the anchorage effect of lap splices, are about 93MPa and 55MPa, respectively. The compressive strength of polymer mortar is 35MPa.

Table 2- Mechanical properties of reinforcement bars

Bar diameter (mm)	Yield strength (MPa)	Yield strain ($\times 10^{-6}$)	Ultimate strength (MPa)	Elastic modulus (MPa)
6.5	335	1806	460	1855
14	355	1828	515	1941
20	375	1947	520	1926

Table 3- Mechanical properties of HSW

HSW diameter (mm)	Single steel filament diameter (mm)	Nominal area (mm^2)	Maximum load (kN)	Ultimate strength (MPa)
6	0.34	12.07	22.30	1847.6
8	0.48	24.05	42.86	1782.1

2.4 Test setup

The experimental setup and loading system have been formalized and fabricated to simulate the boundary condition of beam-column subassemblies, where column and beam ends are considered as the points of contraflexure, as shown in Fig. 4. The cyclic load was applied at the column tip in which the "P-Delta" effect on the column flexural demand can be considered. At the bottom of the column surface, the steel plate was attached to a hinge support using twelve high strength threaded rods. Two ends of the concrete beam were tied to two sets of rigid links through steel pivots that could freely rotate in the plane of the beam-column joint for testing. The rigid links and hinge support, in turn, were fastened to a strong steel I-beam. The latter was mounted to the strong floor using high strength posttensioning rods. The specimens were subjected to combination of vertical and lateral loads, as shown in Fig. 4.The vertical load was applied to the specimens through a vertical hydraulic jack, which was fastened to a slide cart, and then the hydraulic jack can move together with the column tip during the experiment. The vertical load was maintained constant during each test. The lateral load reversal was applied on the column tip in displacement control mode using an MTS actuator supported by the strong wall in the laboratory.

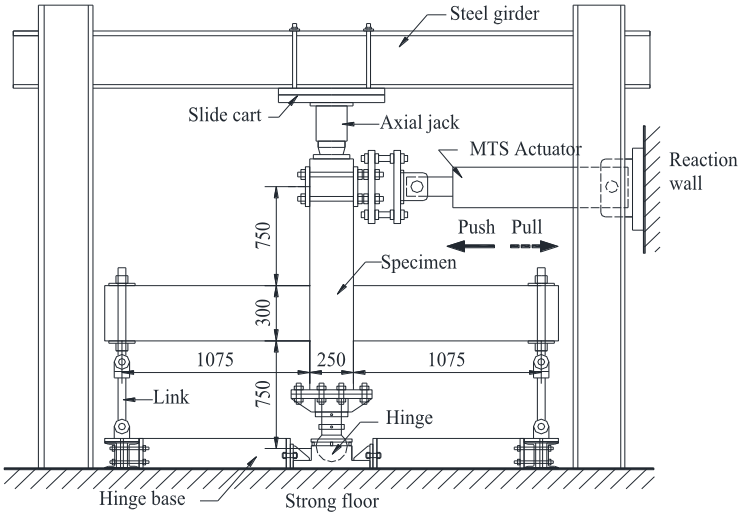

(a) Loading arrangement

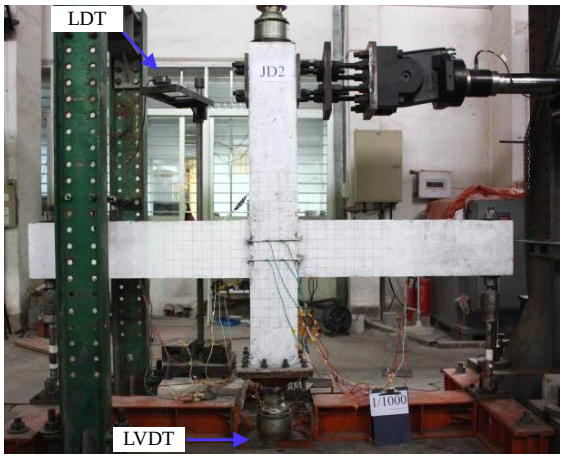

(b) Test rig

Fig. 4- Experimental setup

2.5 Instrumentation

For the measurement of material strain levels of the specimens, electrical-resistance strain gauges were used and placed, as shown in Fig. 5, at different locations of longitudinal and transverse steel reinforcement. The test specimen was instrumented with several measuring instruments. Details of the instrumentation layout are illustrated in Fig. 6. Five pairs of linear voltage displacement transducers (LVDTs) with a range of 50 mm, which were used for measuring deformation, are shown in Fig. 6. LVDT 1-2 were placed diagonally at the panel zone in order to assess the joint shear distortion during the experiment. LVDT 3-8 were placed on each side of the beam/column close to joint to measure the lateral/vertical deflections to obtain the distributions of curvature and rotation in the potential plastic hinge region. LVDT 9-10, attached to top beam bar, were used to obtain the bond-slip of beam end at the face of column. Moreover, the deflections of column tip and the column bottom support were monitored through laser displacement transducer (LDT) with a range of 100 mm and LVDT, respectively, as shown in Fig. 4.

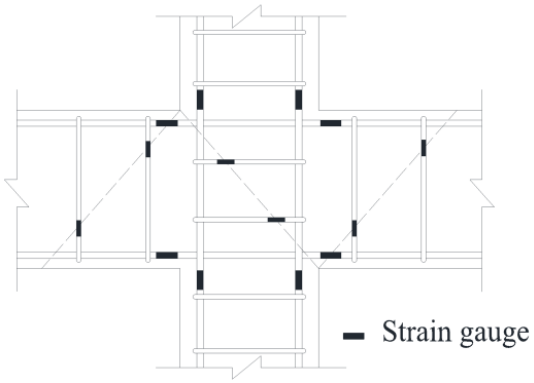

Fig. 5- Layout of strain gauges in joint zone

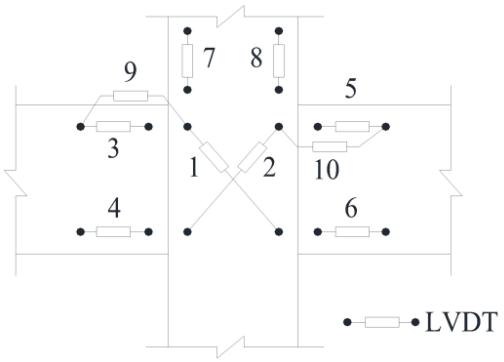

Fig. 6- Layout of LVDTs in joint zone

2.6 Testing Procedure

In the experiment, first, an axial load of a 153.2 kN was applied to the column through the hydraulic jack, and maintained constant during the test. The axial load represents 17% of the axial capacity of the column. To compare the seismic behavior and damage characteristics with respect to critical drift ratio, lateral load was applied on the column tip in displacement control mode throughout the test using the MTS actuator according to the load history, as shown in Fig. 7. Reverse cyclic load is applied in terms of the drift ratio of the beam column subassemblage where the drift ratio δ is calculated as

$$\delta = \Delta / H_c \tag{1}$$

where Δ and H_c are the applied displacement at the column tip and the length between two points of contraflexure of the column, respectively.

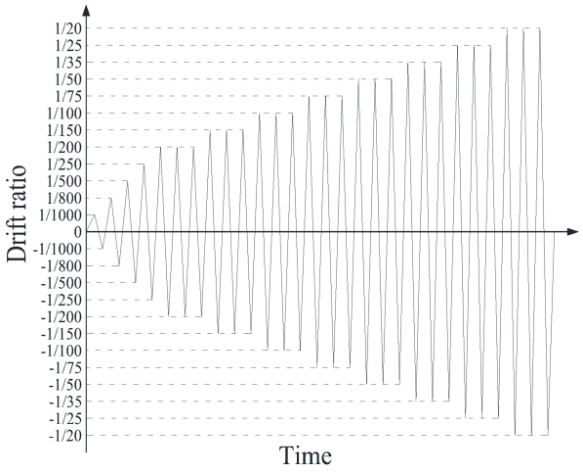

Fig. 7- Loading history

3. Results and discussion

3.1 General observation of the specimens

The typical ultimate failure modes and load-displacement curve of specimens are shown in Fig. 8. Control specimen J1 failed in brittle joint shear as expected. However, the failure mechanism was changed from the joint shear failure in the control specimen to ductile beam flexure mode in the retrofitted specimens, which testifies to the effectiveness of the retrofit scheme.

For the control specimen J1, the first crack occurred in the beam, near the face of the column at a drift ratio of 1/800, and the first crack in the joint panel was recorded at a drift ratio of 1/250. Before yielding of longitudinal beam bars, diagonal shear cracks developed in the joint panel in each loading direction and formed an X-pattern. The column tip load reached its maximum at a drift ratio of 1/50. As the column tip displacement increased, the number and width of cracks also increased. The cover concrete in the joint region began to spall off, and the joint shear capacity deteriorated. A considerable degradation in strength occurred when the drift ratio reached 1/25 which caused the termination of the test.

For the retrofitted specimens, similar to control specimen J1, the first crack was also recorded in the beam at the face of the column at a drift ratio of 1/800. However, the first crack in the joint panel was delayed because of strengthening. As the drift ratio increased, the quantity and width of cracks in the retrofitted joint panel increased but by less than that of control specimen J1 at the same drift ratio. Specimen J2, with two PHSWs around the joint core but without a polymer mortar layer, performed well. The specimen sustained a maximum column tip load of 40.71 kN and reached a ductility factor of about 5.26.

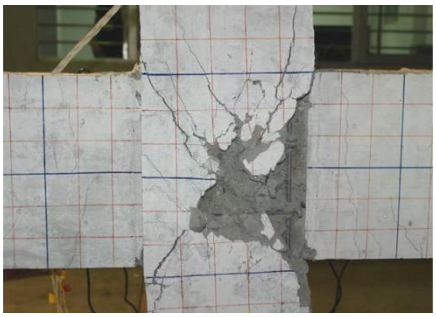

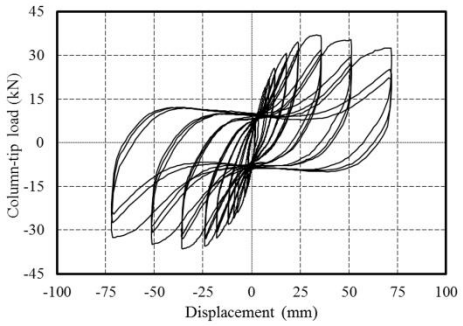

(a) Control specimen J1

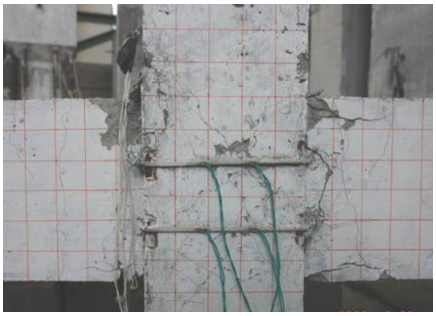

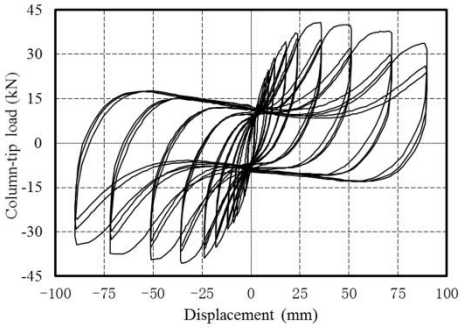

(b) Retrofitted specimen J2

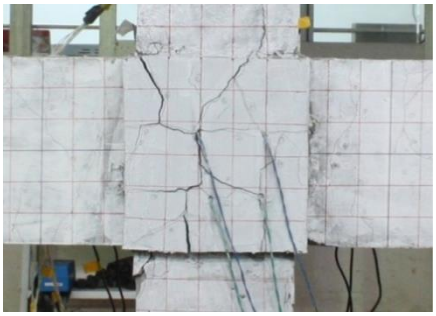

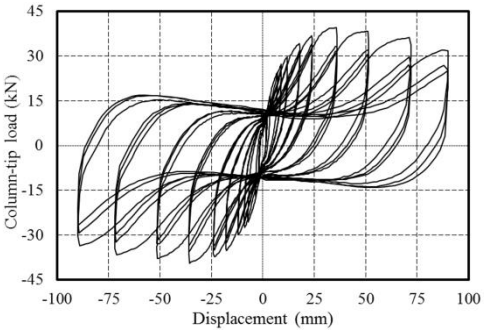

(c) Retrofitted specimen J3

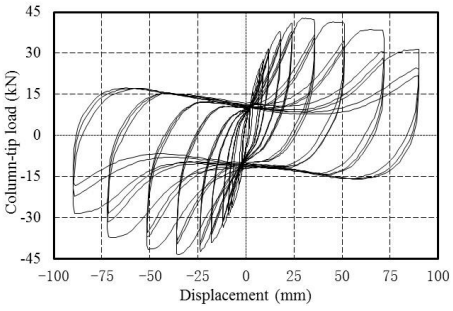

(d) Retrofitted specimen J7

Fig. 8- Typical failure modes mode and load-displacement hysteretic loops

In the test, the longitudinal beam bars yielded. As the concrete in the compression block gradually crushed and spalled off at the face of the column with the corresponding load reduction, a flexural plastic hinge in the beam developed starting from the face of the column. Finally, specimen J2 failed in ductile beam flexural mode. The final failure and crack pattern of the specimen are shown in Fig. 8b. For spatial joint specimens, specimen J7 and specimen J8 have a similar phenomenon. Cracks were localized at the end of the beams. Eventually, the spatial joint specimens J7 and J8 failed in ductile beam flexural mode as shown in Fig. 8d. It's deserved to note that no anchorage failure in lap splice locations of PHSW was observed in the planar joints and spatial joints. Hence the effectiveness of the anchorage scheme has been proven successful.

3.2 Hysteretic behavior

The column tip load versus displacement relationships of typical specimens are illustrated in Fig.8. From the hysteretic loops the strength and stiffness degradation can be observed, and the energy dissipation capacity can also be accounted for. As the hysteretic loops shown in Fig. 8, the retrofitted planar joint specimens almost have the same hysteretic relationship as the control specimen J1 before the drift ratio of 1/250, which indicates that the retrofit scheme has little effect on the original stiffness. For control specimen J1, with the increase of lateral load, the hysteretic loops showed considerable pinching and severe strength degradation, especially after the drift ratio of 1/50. The considerable pinching of the hysteretic loops was primarily attributed to the open and close of diagonal shear cracks developed in the joint during loading and unloading. In the hysteretic loops of retrofitted specimens, considerable pinching after the longitudinal beam bar yielding is observed. That is because of the severe bond-slip of longitudinal beam bars at the face of the column. As compared to control specimen J1, the hysteretic loops of retrofitted specimens showed an improved ductile behavior due to the joint PHSW rehabilitation which provided confinement to the concrete and enhanced the joint shear strength and ductility.

3.3 Load-Displacement envelope

The envelope of the displacement cycles under column tip load is presented in Fig. 9, and the experimental results of the key points for all of the envelope such as yield point, peak load point and ultimate point, are listed in Table 4. The yield point of the specimens is determined corresponding to the yield point of an equivalent elasto-plastic system with the same energy absorption as shown in Fig. 10, and the ultimate point corresponds to the loss of 15% of the peak load of the specimen.

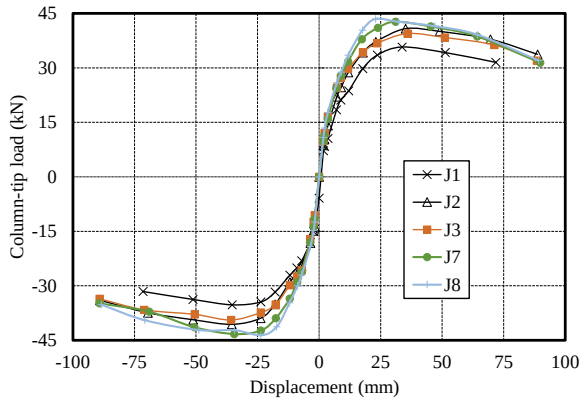

Fig. 9- Load-displacement envelope of specimens

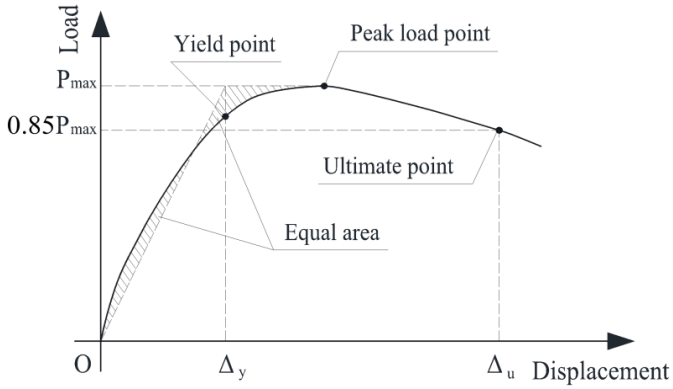

Fig. 10-Characteristic points on load-displacement curve

Comparison of the load-displacement envelope plots in Fig.9 shows significant differences between the performance of control specimen and retrofitted specimens. The retrofitted specimens had a slightly higher yield

load and a much better peak load than that of control specimen J1 due to the joint PHSW retrofit scheme. In the test, contribution of the prestressing level and strengthening ratio to the shear strength of joint hadn't be completely developed owing to the beam flexural mode. Because all the retrofitted specimens failed in beam flexural mode, the peak load of the specimens is mainly governed by the ultimate flexural strength of beam. For spatial joints, the load-displacement envelope of specimen J7 almost coincided with that of specimen J8, which indicates that the anchorage location has no obvious influence on the load-displacement envelope.

Table 4- Characteristic value of the Load-Displacement envelope

Specimen	P_y(kN)	Δ_y(mm)	P_{max}(kN)	Δ_{max} (mm)	P_u(kN)	Δ_u(mm)	$P_{max}/P_{max,1}$	μ_d
J1	30.24	16.14	35.74	34.43	31.31	71.78	1	4.45
J2	33.52	16.02	40.71	35.28	34.60	85.20	1.14	5.31
J3	33.82	15.48	39.43	35.85	33.52	86.01	1.10	5.56
J7	36.18	13.55	43.00	32.81	36.55	75.27	1.20	5.56
J8	36.18	13.64	43.54	23.29	37.01	76.35	1.22	5.60

It can be seen from table 4 that the polymer mortar layer has little influence on the peak load owing to local debonding occurred in the test, comparison of specimens J2 and J3, however, which will enhance the energy dissipation capacity. Hence, steel wire play a main role in producing effective confinement and enhance the shear-resistance capacity of the joint.

3.4 Ductility factor

The displacement ductility factor is defined as

$$\mu_d = \Delta_u / \Delta_y \tag{2}$$

where Δ_y is the horizontal displacement corresponding to the yield point, and Δ_u is the ultimate displacement corresponding to the loss of 15% of the maximum restoring force of the specimen.

The available displacement ductility factors of the tested beam-column joints are given in Table 4. It can be seen from Table 4 that the retrofitted specimens had a lower yield displacement and lower rate of strength deterioration comparing with the control specimen, due to the effective confinement to the joint core using the PHSW scheme. Moreover, the failure mode of retrofitted specimens is changed from brittle joint shear failure to ductile beam flexural failure. In this test, the ductility factor of the retrofitted specimens was enhanced by at least 20%, in comparison with control specimen J1.

3.5 Energy dissipation capacity

The energy dissipation in each cycle is calculated from the area enclosed by the hysteretic loops in the corresponding column tip load displacement cycle. The energy dissipated at different drift ratios were shown in Table 5. Equivalent viscous damping represent the combined effects of elastic and hysteretic damping, which can reflect energy dissipation capacity and pinching degree. The equivalent viscous damping of the test specimens corresponding to the hysteretic response can be computed from the following

$$\xi_{eq} = \frac{1}{4\pi} \cdot \frac{E_{Sto}}{E_{Diss}} \tag{3}$$

where E_{Diss} is the energy loss per cycle and E_{Sto} represents the elastic strain energy stored in an equivalent linear elastic system as shown pictorially in Fig 11. The equivalent viscous damping of the test specimens are calculated as shown in Fig. 11(b).

Table 5- Energy dissipation at different drift ratios

Specimen	Energy dissipation (kN.m)					Total cumulative energy dissipation (kN.m)
	1/75	1/50	1/35	1/25	1/20	
J1	2.19	4.06	6.24	9.04	-	21.53
J2	2.52	4.45	6.93	10.54	13.08	37.52
J3	2.80	4.75	7.27	10.80	13.80	39.43
J7	2.97	5.27	7.82	11.57	13.54	41.16
J8	3.09	5.95	8.49	12.40	15.14	45.08

It can be seen from Table 5 that retrofitted specimens dissipate more energy than control specimen J1 at each cycle. The cumulative energy dissipation increased significantly in retroffited specimens. The test of specimen J1 was terminated when drift ratio reaches 1/25 owing to brittle joint shear failure, so the cumulative energy dissipation was inferior. Meanwhile, as shown in Fig. 11, retrofitted specimens have a higher equivalent viscous damping than control specimen, which indicates that the hysteretic loops of retrofitted specimens at each cycle were well-rounded because of the beam flexural failure compared with the control specimen.

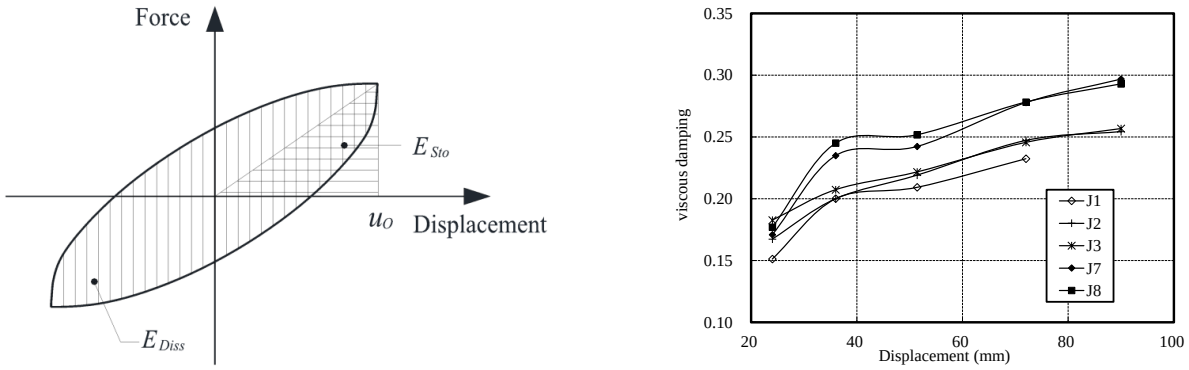

(a) Dissipated and stored forces for viscous damping (b) Equivalent viscous damping ratio

Fig. 11. Equivalent viscous damping ratios of test specimens

4. Conclusion

An innovative technique is presented for the seismic retrofit of reinforced concrete beam-column joints using prestressed high-strength steel wires (PHSW). This method provides a simple and efficient, yet economic, means of improving the seismic performance and enhancing the shear strength of reinforced concrete beam-column joints. Six large-scale interior beam-column joint assemblies were tested under reversed cyclic loading, where five were strengthened using PHSW and one was un-retrofitted as a control specimen. Based on this experimental investigation, the following general conclusions can be drawn.

(1) The control specimen J1 without retrofitted in the joint area showed a high rate of strength and stiffness deterioration and low energy dissipation capacity due to the brittle shear failure of the joint.

(2) The proposed method for the seismic retrofit of RC beam-column joints using prestressed high-strength steel wires has proven successful for effectively enhancing the shear strength of RC beam-column joints and their energy dissipation capacity as well as the ductility ability.

(3) All retrofitted specimens failed in a ductile mode of beam flexural failure rather than a brittle mode of joint shear failure in the control specimen without retrofitting, exhibiting that energy dissipation characteristics and ductility of the retrofitted specimens are much superior to those of the un-retrofitted specimen.

(4) No anchorage failure occurred at the lap splice locations of steel wires. Meanwhile, anchorage location has no obvious influence on the seismic performance of joints. Hence, the anchorage scheme involving steel wire clips and injection epoxy glue worked well.

5. Acknowledgement

The study presented in this paper was funded by National Science Found of China under grant No. 51208219, and Science Found of Fujian province under grant No. 2016J01240.

References

[1] Engindeniz M, Kahn LF, Zureick A-H (2005): Repair and strengthening of reinforced concrete beam-column joints: State of the art. *ACI structural journal*, **102**(2), 1-14.
[2] Alcocer SM (1993): RC frame connections rehabilitated by jacketing. *Journal of Structural Engineering*, **119**(5), 1413-1431.
[3] Pimanmas A, Chaimahawan P (2010): Shear strength of beam–column joint with enlarged joint area. *Engineering structures*, **32**(9), 2529-2545.
[4] Alcocer SM, Jirsa JO (1993): Strength of reinforced concrete frame connections rehabilitated by jacketing. *ACI Structural Journal*, **90**(3), 249-261.
[5] Ghobarah A, Aziz T, Biddah A (1997): Rehabilitation of reinforced concrete frame connections using corrugated steel jacketing. *ACI structural journal*, **94**(3), 283-294.
[6] Antonopoulos CP, Triantafillou TC (2003): Experimental investigation of FRP-strengthened RC beam-column joints. *Journal of composites for construction*, **7**(1), 39-49.
[7] Akguzel U, Pampanin S (2012): Assessment and design procedure for the seismic retrofit of reinforced concrete beam-column joints using FRP composite materials. J*ournal of Composites for Construction*, **16**(1), 21-34.
[8] Biddah A, Ghobarah A, Aziz TS (1997): Upgrading of nonductile reinforced concrete frame connections. *Journal of Structural Engineering*, **123**(8), 1001-1010.
[9] Misir I, Kahraman S (2013): Strengthening of non-seismically detailed reinforced concrete beam–column joints using SIFCON blocks. *Sadhana*, **38**(1), 69-88.
[10] Munawar AH, Robert GC (2004): Experimental study on the seismic performance of externally confined reinforced concrete columns. Proceedings of the 13th WCEE, Vancouver, B.C., Canada.
[11] Saatcioglu M, Yalcin C (2003): External prestressing concrete columns for improved seismic shear resistance. *Journal of Structural Engineering*, **129**(8), 1057-1070.
[12] Guo ZX, Jie Z, Li CL (2009): Seismic strengthening of rectangular RC columns using prestressing steel jackets. *China Civil Engineering Journal*, **42**(12), 112-117.